A PASSIVE RFID TAG FOR BIOMASS TRACKING

Amjad Ali[1], Roderick Mackenzie[2], Ed Lester[3], Orla Williams[3], Steve Greedy [1].
[1] School of Electrical Engineering, University of Nottingham, Nottingham, UK, Amjad.Ali@nottingham.ac.uk.
[2] School of Mechanical Engineering, University of Nottingham, Nottingham, UK.
[3] Advanced Materials Research Group, Faculty of Engineering, University of Nottingham, Nottingham, UK.

***Abstract*—This paper presents the design for a low cost miniaturized chipless RFID tag for short-range biomass tracking and monitoring purposes. The concentric hexagonal geometry and angular stability, leading to higher data capacity are the novel aspects of the proposed design, which can encode four data bits within a compact size of 1 cm radius. The designed is capable of encoding 2^n unique IDs in a 4-to-9 GHz frequency band, where n is the number of etched slots. The angular stability makes this tag readable from any angle in biomass. Moreover, this chipless RFID tag has no hazard as compared to battery-based active tags during biomass combustion processes.**

***Index Terms*—antennas, biomass, chipless RFID, reader, tag, tracking.**

I. INTRODUCTION

Radio-Frequency Identification (RFID) is a wireless data capturing technology, which utilises radio-frequency signals to automatically identify of remotely located objects [1]. Due to their simplicity, low cost and data sensing ability, this technology has been widely adopted in various sectors such as industry, academia, commerce, telecommunication, tracking systems, access control, and health monitoring [1]–[3]. RFID technology started its journey from World War II, 1941, when a British air-jet pilot performed a rollover in his jet, and a shift in the reflected radar signals were observed at Pearl Harbor lab [4]. After that, in 1948, Stockman proposed it as RFID technology, that a varying load on the tag antenna produces a varying reflected power, which can be used for identification [5]. Commercial use of this technology started in 1980s, and enormous range of applications for this technology has been observed in recent decades [6]. RFID technology has found application in broad area of tracking, security, access and control. More specific examples of their use: Australian industries use RFID tags for tracking their products across the globe [7]; tags embedded in ID cards are used for security purposes, access and control [1]–[3]; tags are embedded within goods sold throughout shopping malls to prevent theft [6]. The above examples and many more applications of RFID technology provide one pathway to the realization of Internet of Things (IoT) [3].

Existing RFID technology is categorized into active and passive RFID tags, shown in Fig. 1. Where active tags assisted with on board battery and can be used for long read range (up to 500 m) with high coding capacity and other necessary information [8]. Active tags periodically transmit their data signal towards the reader. The reader receives

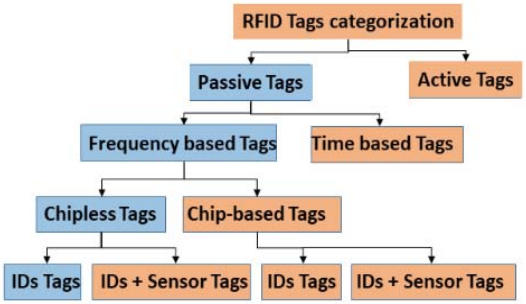

Fig. 1. Categorization and Development of RFID tags technology

-these signals and performs the required operation such as cross-referencing to the existing data and updating tags table etc. However, it is not a cheap technology due to the presence of expensive lithium cell batteries [3].

In contrast, the on-board battery in the passive tags is replaced by a mechanism, in which the reader transmits a high energy signal toward the tag. The tag uses it for its operation and responses back. Therefore, this technology has become more promising in terms of low cost, small size and environmentally friendliness. The chipless RFID technology could be further categorized into, time-based and frequency-based tags. In time-based tags, the time difference of transmitted and reflected signals from the tag is monitored. Each tag has its particular time difference, which is used as encoded data [9]. In the frequency-based tags, the reflected back spectral signatures from the tag are monitored, which are then used as encoded data [9]. These frequency-based tags can be further divided into two classes, chip-based, and chipless tags. The chip-based RFID tag consists of an integrated chip (IC) to store the data and an antenna to act as a transceiver [1]. The antenna is used to collect RF power from the reader transmitted signal, and couple it to IC for operation. However, the chip-based tags have still a high cost and complex fabrication due to the presence of the IC [1]. A lot of research effort has been undertaken to reduce the cost and complexity of the RFID tags by storing the information data without a storage device, which has resulted in chipless RFID tags. These tags store the data in its geometrical structure, which consists of backscatters or resonators. These resonators reflect back a linearly polarized wave in particular spectral signatures, which used as identification codes. For example, R. Dinesh et al reported a tag with eight straight line resonators, which produces eight corresponding frequency signatures [10]. In the last two decades,

researchers have been digging out different geometrical structures for chipless RFID tags. This has resulted in a variety of geometrical structures for resonators such as straight-line [11], spiral [12], 'C' and 'U' shape [3][13][14], circular and half-circle [15], elliptical [2], square [16], triangular [17], E-shaped micro strip [18], and ladder-shaped [19].

In this work, we present for the first time a high coding capacity, inexpensive, miniaturized, and easy to fabricate chipless RFID tag, which is based on nested concentric hexagonal resonators (NCH) that encodes four data bits in a compact dimension of 2.6 cm^2. The NCH shape geometry has not been reported to-date and seeks to improve read range, angular stability, and code density. There is channel noise and electrical noise due to thermal excitation of electrons in a real-time environment while tracking the chipless tag [20]. To overcome this hurdle, high magnitude resonances are achieved. Moreover, the resonances of this NCH chipless RFID tag are clearer and sharper compared to the report in [12], [20]. The paper outline is:

- Application of proposed tag.
- Design and operation of the passive RFID tag.
- Results and discussion.
- Conclusion.

II. Application of Proposed RFID Tag

According to the Climate Change Act of 2008, the United Kingdom is targeting to reduce at least 80% of the greenhouse gas (GHG) emission by 2050 [21]. Regarding this, renewable energy (RE) like biomass fuel could play a major role in the reduction of GHG emissions. As per this much future demand of biomass pellets, the needs of its tracking and monitoring are aroused. For this matter, fully passive chipless RFID tag has been suggested as an approach to biomass pellet tracking and monitoring purposes. Moreover, for auto-tracking, each tag needs a unique ID to distinguish them from each other. Considering these important requirement an NCH chipless RFID tag has been designed and simulated.

III. Design and Operation of Passive RFID Tag

There are two types of resonators in chipless RFID tags, a metallic resonator, and a hollow slot. In the case of the metallic resonator, a conductive resonator is designed over substrate which gives a dip at a particular frequency [22]. While the hollow slot operates as a band-pass filter. In this type of chipless RFID tags, a hollow slot is etched in thick copper cladding. This hollow slot allows those frequencies to pass by, whose wavelengths are matched with the slot length and width, while the rest of frequencies is reflected back [3]. The pass-by frequencies make a sharp resonance in reflected back spectrum, which is treated as code. This data encoding mechanism is used in the presented NCH RFID tag design.

The proposed tag uses Roger RT6002 as a substrate of a 1 cm hexagonal radius with a thickness of 1.524 mm, dielectric permittivity ε_r=2.94, and 0.0012 tangent loss. The tag is designed by etching hollow slots in 0.035 mm thick copper cladding. Initially, the horizontal waves of 0 dBsm power fall on a plane tag. The RCS response shows a smooth curve with 25 dBsm loss as compared to the transmitted power. Then a single hexagonal shape slot was etched, shown in Fig. 2. The slot radius R_s was calculated using (1) for particular frequency f_{res}. Here 'C' is the speed of light and 'ε_r' is the relative permittivity of the substrate used. By using (1), a hexagonal slot of radius 5.4 mm was calculated for a resonance frequency of 6.35 GHz. An RCS response with a spectral dip of 28 dBsm magnitude was achieved, shown in Fig. 2.

$$R_s = \frac{C}{2\pi f_{res}}\sqrt{\frac{2}{\varepsilon_r+1}} \quad (1)$$

Thus, it can be used as a 1-bit data encoding chipless RFID tag. Where the possible IDs are '1' when the slot is present and '0' when the tag has no slot. Moreover, if the hollow slot's width is increased, the resonance or band-pass filter will be wider. The comparison of 0.2 mm thin and 3 mm thick hollow slot is shown in Fig. 3. Where thin slot allows 200 MHz and thick slot allows 1200 MHz band of frequencies at -40 dBsm. From high data capacity point of view, the hollow slot width is kept to 0.2 mm to achieve a maximum number of resonances in a compact frequency band. The proposed tag data capacity was further increased by following the same designing approach, and three nested

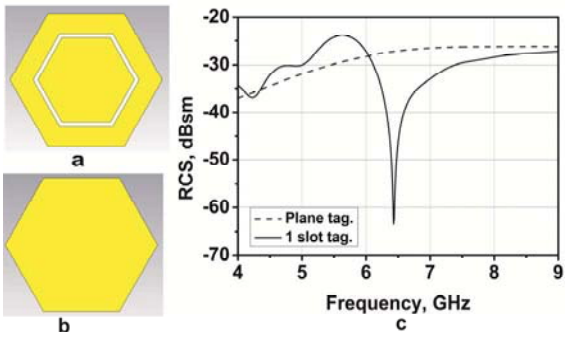

Fig. 2. (a) a single hollow slot with radius 5.6 mm and width 0.2 mm (b) a plane tag, and (c) Simulated RCS response of tags 'a' and 'b'.

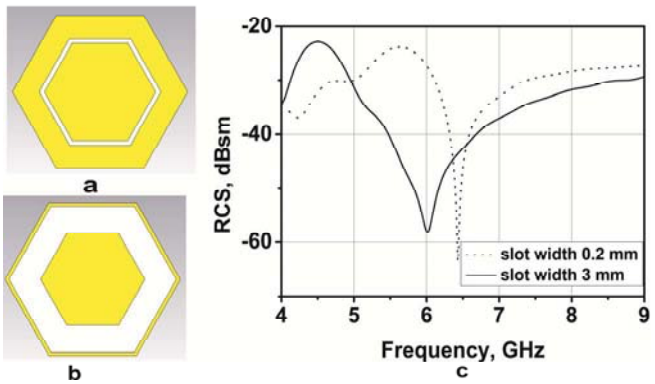

Fig. 3. Hollow slot behaving as a band-pass filter, (a) slot width 0.2 mm, (b) slot width 3 mm, (c) at -40 dBsm 'tag a' allows 200 MHz band of frequencies while 'tag b' allows 1200 MHz band of frequencies.

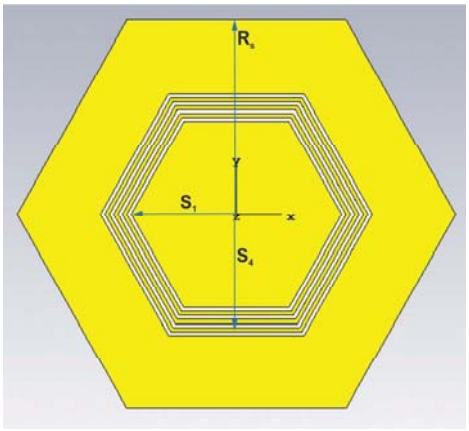

Fig. 4. 4-bit NCH chipless RFID tag has radius R_S= 10 mm, interior slot radius is S_1= 5 mm, and exterior slot radius is S_4=6.2. The slots width and spacing are 0.2 mm.

TABLE I. DIMENSION OF PROPOSED TAG, ALL HOLLOW NCH SLOT WIDTH AND SPACING ARE KEPT TO 0.2 MM.

Slot SX	Radius (mm)	Frequency (GHz)
S_1	5	7.82
S_2	5.4	6.25
S_3	5.8	5.65
S_4	6.2	5.43

-concentric hexagons (NCH) were added, shown in Fig. 4. Yielding a 1.53-bit/cm^2 of presented 4 bit tag, which maybe further increased to 18 bits with the same cross sectional area resulting in 6.92-bits/cm^2. In comparison the device in [2] has a 2.74-bit/cm^2 data encoding capacity. The slot's width and space was kept at 0.2 mm. The optimized tag substrate has a radius R_s=10 mm, the innermost slot has a radius of S_1=5 mm and the outermost slot has a radius S_4=6.2 mm. The detail tag dimensions and resonance frequencies are summarized in Table I.

IV. RESULTS AND DISCUSSION

The simulations of the proposed tag were performed in the commercially available electromagnetic simulation software CST Studio [3]. The tag was excited by a horizontal plane wave with a 0 dBsm power. An RCS probe was placed at the far-field at different distances d=10 cm and observed the backscattered spectral signatures. This distance was calculated using (2).

$$d = \frac{2D^2}{\lambda} \quad (2)$$

$$D = \frac{3\sqrt{3}}{2} a \quad (3)$$

In (2) 'λ' is the central frequency wavelength of the operating band and 'D' is the maximum dimension of the tag. In hexagonal shape tag, the dimension 'D' is calculated by using the (3), where 'a' is the hexagonal substrate corner length. According to the (1), the NCH slot radius (R_s) is inversely proportional to its resonating frequency (f_{res}) which has been observed in Fig. 5, where two tags, NCH tag-1, and NCH tag-2, are made. The inner slot has a 5 mm radius, which has the least length in both tags. The second slot of NCH tag-2 has larger radius of 5.4 mm. Theoretical results of Fig. 5 show that the smaller slot of both tags have spectral signature at higher frequency, and the larger slot of NCH tag-2 has spectral signature at lower frequency and vice versa. Thus, the RCS comparison of these two tags supports (1). In contrast, if any two slots were shortened, then they provide one wide spectral signature, which is shown in Fig. 3. Furthermore, the simulated RCS response of four-bit IDs encoding NCH tag is shown in Fig. 6, where each spectral signature B1, B2, B3, and B4 have 1:1 correspondence with NCH slot S_1, S_2, S_3, and S_4. From a coding point of view, B4 and B1 are treated as most significant bit (MSB), and least significant bit (LSB) respectively. The simulation shows that the tag can be readable up-to 1m distance. Moreover, the suggested tag has angular stability for all 'ϕ' angles except at

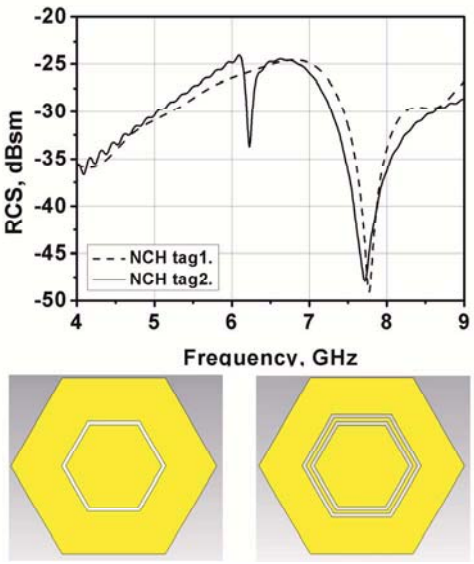

Fig. 5. The smaller slot of both tags, NCH tag-1, and NCH tag-2 have a spectral signature at a higher frequency while larger slot of NCH tag-2 has spectral signature at lower frequency.

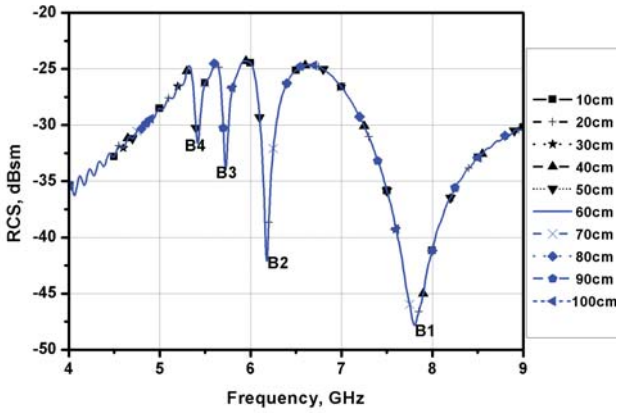

Fig. 6. Simulated RCS response of 4-bit NCH tag.The RCS probe is placed at various distance from 10 cm to 100 cm.

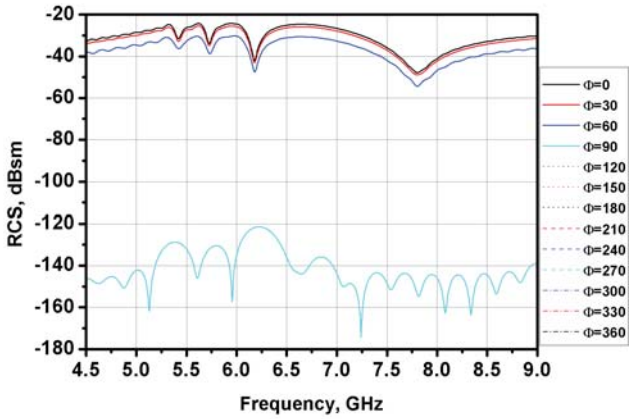

Fi. 7. Angular stability for all • angles except at 90º and 270º.

90 and 270. Fig. 7 shows angular stability, where a drastic downward shift and noise is observed at •= 90º and 270º. Furthermore, simulation also shows that the angle pattern is repeated after 90º. This NCH chipless RFID tag has a novel 3D geometry that results in a clearer RCS response as compared to [12], [20].

V. Conclusion

A high coding capacity tag, with a novel geometry is designed on a low-cost Roger substrate for biomass tracking and monitoring purposes. This novel tag has a unique geometrical NCH structure in a small form factor 2.6 cm^2. This smart tag is capable to encode 2^n unique identification IDs in a compact RF band of 4 to 9 GHz. Moreover, it has angular stability for all ϕ angles except 90º and 270º, where a drastic downward shift is observed. Additionally, this tag has grindable and combustible properties during biomass combustion, and so is easily disposed of.

The future aim of this research project is tracking Biomass pellets alongside with sensing its ambient humidity, temperature, and CO_2 level by using a fully passive chipless RFID tags. For this purpose, the code density of the proposed NCH-RIFD tag will be increased, and sensing ability will be added.

Acknowledgment

I would like to thank the government of Pakistan for the support and funding for this research. This work was supported through the provision of a cooperation license for CST Studio Suite provide by Dassault Systems (https://www.3ds.com/products-services/simulia/products/cst-studio-suite/).

References

[1] S. Preradovic and N. C. Karmakar, "Chipless RFID: Bar code of the future," *IEEE Microw. Mag.*, vol. 11, no. 7, pp. 87–97, 2010.

[2] I. Jabeen, A. Ejaz, A. Akram, Y. Amin, J. Loo, and H. Tenhunen, "Elliptical slot based polarization insensitive compact and flexible chipless RFID tag," *Int. J. RF Microw. Comput. Eng.*, p. e21734, 2019.

[3] A. Ali, S. I. Jafri, A. Habib, Y. Amin, and H. Tenhunen, "RFID Humidity Sensor Tag for Low-cost Applications.," *Appl. Comput. Electromagn. Soc. J.*, vol. 32, no. 12, 2017.

[4] D. M. Dobkin, *The rf in RFID: uhf RFID in practice*. Newnes, 2012.

[5] H. Stockman, "Communication by means of reflected power," *Proc. IRE*, vol. 36, no. 10, pp. 1196–1204, 1948.

[6] Y. Bai, "Development of a WiFi and RFID based indoor location and mobility tracking system," 2016.

[7] J. P. T. Mo, Q. Z. Sheng, X. Li, and S. Zeadally, "RFID infrastructure design: a case study of two Australian RFID projects," *IEEE Internet Comput.*, vol. 13, no. 1, pp. 14–21, 2009.

[8] J. Wang, O. Abari, and S. Keshav, "Challenge: RFID Hacking for Fun and Profit," in *Proceedings of the 24th Annual International Conference on Mobile Computing and Networking*, 2018, pp. 461–470.

[9] S. Dey *et al.*, "Smart Sensing."

[10] R. Dinesh, P. V Anila, C. M. Nijas, M. Sumi, and P. Mohanan, "Modified open stub multi-resonator based chipless RFID tag," in *2014 XXXIth URSI General Assembly and Scientific Symposium (URSI GASS)*, 2014, pp. 1–4.

[11] M. A. Islam and N. Karmakar, "A compact printable dual-polarized chipless RFID tag using slot length variation in'I'slot resonators," in *2015 European Microwave Conference (EuMC)*, 2015, pp. 96–99.

[12] S. Preradovic and N. C. Karmakar, "Design of fully printable planar chipless RFID transponder with 35-bit data capacity," in *2009 European Microwave Conference (EuMC)*, 2009, pp. 13–16.

[13] A. Vena, E. Perret, and S. Tedjini, "Chipless RFID tag using hybrid coding technique," *IEEE Trans. Microw. Theory Tech.*, vol. 59, no. 12, pp. 3356–3364, 2011.

[14] E. M. Amin, J. K. Saha, and N. C. Karmakar, "Smart sensing materials for low-cost chipless RFID sensor," *IEEE Sens. J.*, vol. 14, no. 7, pp. 2198–2207, 2014.

[15] S. Zeb, A. Habib, Y. Amin, H. Tenhunen, and J. Loo, "Green Electronic Based Chipless Humidity Sensor for IoT Applications," in *2018 IEEE Green Technologies Conference (GreenTech)*, 2018, pp. 172–175.

[16] D. Lu, Y. Zheng, M. Schüßler, A. Penirschke, and R. Jakoby, "Highly sensitive chipless wireless relative humidity sensor based on polyvinyl-alcohol film," in *2014 IEEE Antennas and Propagation Society International Symposium (APSURSI)*, 2014, pp. 1612–1613.

[17] S. Rauf, M. A. Riaz, H. Shahid, M. S. Iqbal, Y. Amin, and H. Tenhunen, "Triangular loop resonator based compact chipless RFID tag," *IEICE Electron. Express*, pp. 14–20161262, 2017.

[18] M. Sumi, R. Dinesh, C. M. Nijas, S. Mridula, and P. Mohanan, "High bit encoding chipless RFID tag using multiple E shaped microstrip resonators," *Prog. Electromagn. Res.*, vol. 61, pp. 185–196, 2014.

[19] M. Martinez and D. Van Der Weide, "Circular polarization on depolarizing chipless RFID tags," in *2016 IEEE Radio and Wireless Symposium (RWS)*, 2016, pp. 145–147.

[20] R. Rezaiesarlak and M. Manteghi, "A space–time–frequency anticollision algorithm for identifying chipless RFID tags," *IEEE Trans. Antennas Propag.*, vol. 62, no. 3, pp. 1425–1432, 2013.

[21] A. L. Stephenson and D. J. MacKay, "Life cycle impacts of biomass electricity in 2020," *UK Dep. Energy Clim. Chang.*, 2014.

[22] S. Dey and N. C. Karmakar, "Towards an inexpensive paper based flexible chipless RFID tag with increased data capacity," in *2017 Eleventh International Conference on Sensing Technology (ICST)*, 2017, pp. 1–5.